Journal of Computational Physics **153,** 467–487 (1999)
Article ID jcph.1999.6286, available online at http://www.idealibrary.com on IDEAL®

A Conservative Spectral Method for Several Two-Dimensional Nonlinear Wave Equations

B.-F. Feng,*,† T. Kawahara,*,‡ and T. Mitsui§

*Department of Aeronautics and Astronautics, Graduate School of Engineering, Kyoto University, Kyoto 606-8501, Japan; and §Graduate School of Human Informatics, Nagoya University, Nagoya 464-8601, Japan
E-mail: †feng@impact.kuaero.kyoto-u.ac.jp; ‡kawahara@impact.kuaero.kyoto-u.ac.jp; §a41794a@nucc.cc.nagoya-u.ac.jp

Received December 14, 1998; revised May 4, 1999

A conservative spectral method is proposed to solve several two-dimensional nonlinear wave equations. The conventional fast Fourier transform is used to approximate the spatial derivatives and a three-level difference scheme with a free parameter θ is to advance the solution in time. Our time discretization is semi-implicit in the sense that the linear terms are treated implicitly while the nonlinear terms are evaluated only by previous time levels, and thus treated explicitly. However, the cost of the algorithm is no greater than that of a fully explicit method because the linear boundary value problem that must be solved at each time step is almost trivial in a spectral spatial discretization. A linear stability analysis shows that the method leads to a less restrictive stability condition than the corresponding explicit one. The method is conservative and the ratio of the numerical dispersion to the physical dispersion is of the order $O(\Delta t^2)$. Applications of our method to the Kadomtsev–Petviashvili and the Zakharov–Kuznetsov equations exhibit excellent results.

Key Words: conservative spectral method; linear stability analysis; numerical dispersion; Riemann theta-function solution; lump-type soliton; N-phase solution; quasi-soliton.

1. INTRODUCTION

The numerical solution of nonlinear wave equations has been the subject of many studies over the past three decades. Although many numerical schemes have been proposed for some well-known one-dimensional equations, such as the Korteweg–de Vries (KdV) equation [4, 6, 7, 20, 23, 25, 28] and the nonlinear Schrödinger (NLS) equation [10, 12, 21, 27], there is little numerical analysis literature for the multi-dimensional nonlinear wave equations. Usually, an extension of a numerical method for the one-dimensional nonlinear equations to the multi-dimensional case is a difficult problem and raises a more restrictive stability

0021-9991/99 $30.00

condition. Wineberg *et al.* proposed an implicit spectral method for wave propagation problems with applications to the KdV and the Kadomtsev–Petviashvili (KP) equations [26], but their method has the disadvantage of having to solve the nonlinear equations via iterative procedure at every time step.

We note that the third- and the fifth-order KdV equations possess the special features that the higher order spatial derivatives arise only in the linear part, and the nonlinear part contains at most terms of u and u_x, and give a conservative spectral method for the third- and the fifth-order KdV equations [3]. Actually, some typical two-dimensional nonlinear wave equations share the same properties as the third- and the fifth-order KdV equations. Examples are the KP equation

$$\left(u_t + (3u^2)_x + u_{xxx}\right)_x - 3\sigma^2 u_{yy} = 0, \tag{1}$$

and the Zakharov–Kuznetsov (ZK) equation

$$u_t + (3u^2)_x + \Delta u_x = 0, \tag{2}$$

where σ^2 is a real constant and $\Delta \equiv \partial_x^2 + \partial_y^2$ is the two-dimensional Laplacian.

The KP equation may be thought of as a two-dimensional analog of the KdV equation. It is one of the classical prototype problems in the field of exactly solvable equations, and arises in physical contexts of plasma physics and surface water waves.

The ZK equation can be thought of as another form of a two-dimensional generalization of the KdV equation. It was first derived by Zakharov and Kuznetsov to describe nonlinear ion-acoustic waves in a magnetized plasma [29]. In the purely dispersive limit, a variety of physical phenomena are governed by Eq. (2), for example, the long waves on a thin liquid film [14, 24], the Rossby waves in rotating atmosphere [17], and the isolated vortex of the drift waves in three-dimensional plasma [16]. Unlike the KP equation, the ZK equation has no closed form of analytical solutions.

In this paper, we extend our conservative spectral method for the third- and the fifth-order KdV equations to several two-dimensional nonlinear wave equations. Although our analysis is expressed for the above two typical equations, it can be applied to other two-dimensional nonlinear wave equations straightforwardly as well.

Our general framework for numerical approximations can be described as follows: we employ the standard spectral methods (fast Fourier transform, FFT) for the spatial discretization of the equations, while for the time integration we use a three-level difference scheme with a free parameter θ for the linear terms and the leapfrog scheme for the nonlinear terms. Since we employ the leapfrog method for the nonlinear part, it should be stressed that we avoid solving the nonlinear algebraic equations.

This paper is arranged as follows: In Section 2, we propose a conservative spectral method for the two-dimensional nonlinear wave equations. Section 3 is devoted to the analyses of the scheme with respect to linear stability, accuracy, and numerical dispersion. Numerical experiments with various initial conditions for the KP and the ZK equations are reported in Section 4. Comments and conclusions are contained in Section 5.

2. A SPECTRAL METHOD FOR NONLINEAR DISPERSIVE WAVE EQUATIONS

2.1. Notations and Definitions

We restrict ourselves to Eqs. (1)–(2) of finite spatial domain with periodic boundary conditions. This is a standard procedure in dealing with wave phenomena. Consequently

we work on a periodic domain $\Omega = [0, W_x] \times [0, W_y]$. First, we introduce some notations for the discrete Fourier transformation (DFT). We assume that the domain in the x-direction is equidiscretized, with spacing $\Delta x = W_x/L$, while the domain in the y-direction is also equidiscretized, with spacing $\Delta y = W_y/M$. We assume L and M are even integers. On the grid points $(x_l, y_m) = (l\Delta x, m\Delta y)$ of the domain Ω with $l \in \{0, 1, \ldots, L-1\}$ and $m \in \{0, 1, \ldots, M-1\}$, the solution value $u(x_l, y_m, t)$ is approximated as $u_{l,m}(t)$. Let the corresponding spectral variables be denoted $\xi_p = 2\pi p/W_x$ and $\eta_q = 2\pi q/W_y$ with $p \in \{-L/2, \ldots, -1, 0, 1, \ldots, L/2\}$ and $q \in \{-M/2, \ldots, -1, 0, 1, \ldots, M/2\}$. Then DFT is given by

$$\hat{u}_{p,q} = \mathcal{F}u_{l,m} = \sum_{l=0}^{L-1}\sum_{m=0}^{M-1} u_{l,m} e^{-\mathrm{i}(\xi_p x_l + \eta_q y_m)}, \qquad p = -\frac{L}{2}, \ldots, -1, 0, 1, \ldots, \frac{L}{2} - 1,$$

$$q = -\frac{M}{2}, \ldots, -1, 0, 1, \ldots, \frac{M}{2} - 1.$$

The corresponding inverse DFT is defined as

$$u_{l,m} = \mathcal{F}^{-1}\hat{u}_{p,q} = \frac{1}{LM}\sum_{p=-L/2}^{L/2-1}\sum_{q=-M/2}^{M/2-1} \hat{u}_{p,q} e^{\mathrm{i}(\xi_p x_l + \eta_q y_m)},$$

$$l = 0, 1, \ldots, L-1, \qquad m = 0, 1, \ldots, M-1.$$

We employ, of course, the FFT for the DFT and its inverse, and thus L and M are the powers of 2.

2.2. Spectral Method

The Fourier transformation converts Eqs. (1) and (2) into

$$\hat{u}_t + \mathrm{i}\xi\mathcal{F}(3u^2) - \mathrm{i}(\xi^3 + 3\sigma^2\eta^2/\xi)\hat{u} = 0 \tag{3}$$

and

$$\hat{u}_t + \mathrm{i}\xi\mathcal{F}(3u^2) - \mathrm{i}(\xi^3 + \eta^2\xi)\hat{u} = 0, \tag{4}$$

respectively. Usually, an explicit numerical ordinary differential equation (ODE) solver to Eqs. (3)–(4) suffers from a restrictive stability condition on the time step due to the existence of dispersive terms in Eqs. (1)–(2). Implicit methods may allow one to avoid the severe time step restriction, but they are too costly. We therefore make a compromise.

For the time integration of Eqs. (3)–(4), we employ a symmetric three-level difference method for the linear terms and the leapfrog method for the nonlinear terms, which can be written as

$$\frac{\hat{u}^{n+1} - \hat{u}^{n-1}}{2\Delta t} + \mathrm{i}\xi\mathcal{F}((3u^n)^2) - \mathrm{i}(\xi^3 + 3\sigma^2\eta^2/\xi)[\theta(\hat{u}^{n+1} + \hat{u}^{n-1}) + (1 - 2\theta)\hat{u}^n] = 0 \tag{5}$$

for the KP equation and

$$\frac{\hat{u}^{n+1} - \hat{u}^{n-1}}{2\Delta t} + \mathrm{i}\xi\mathcal{F}((3u^n)^2) - \mathrm{i}(\xi^3 + \eta^2\xi)[\theta(\hat{u}^{n+1} + \hat{u}^{n-1}) + (1 - 2\theta)\hat{u}^n] = 0 \tag{6}$$

for the ZK equation, where θ is a free parameter of the method and the superscript denotes the time level.

In addition, we give the scheme by Wineberg *et al.* (hereafter referred to as the Wineberg scheme). They employ the Crank–Nicolson scheme for the temporal discretization, to give

$$\frac{\hat{u}^{n+1}-\hat{u}^n}{\Delta t}+\frac{1}{2}\mathrm{i}\xi(\mathcal{F}((3u^n)^2)+\mathcal{F}((3u^{n+1})^2))-\frac{1}{2}\mathrm{i}(\xi^3+3\sigma^2\eta^2/\xi)[(\hat{u}^{n+1}+\hat{u}^n)]=0. \quad (7)$$

To solve this nonlinear equations, the iteration procedure

$$\hat{u}^{n+1,0}=\hat{u}^n \quad (8)$$

$$\hat{u}^{n+1,r+1}=\left(1-\mathrm{i}\frac{\Delta t}{2}(\xi^3+3\sigma^2\eta^2/\xi)\right)^{-1}\left(\hat{u}^n-\frac{\Delta t}{2}[\mathrm{i}\xi(\mathcal{F}((3u^n)^2)+\mathcal{F}((3u^{n+1,r})^2))-\mathrm{i}(\xi^3+3\sigma^2\eta^2/\xi)\hat{u}^n]\right) \quad (9)$$

is employed for $r=0,1,\ldots,R-1$, where R is the iteration number in each time step.

Since we use three time levels in Eqs. (5) and (6), we need one extra initial approximate solution vectors. These can be obtained from a certain one-step spectral method with the same order in the temporal discretization. The schemes (5) and (6) are apparently semi-implicit, but the computation can be implemented explicitly. We stress that in each time step only twice are FFTs required. Thus, we can expect that our method is more efficient than the method (9).

2.3. Features of Our Method

Spectral methods, or, more strictly speaking, pseudospectral methods, have been extensively studied and widely applied. We refer the interested reader to monographs by Gottlieb and Orszag [15], Boyd [1], and Fornberg [5], and references cited therein. For instance, the FFT pseudospectral method has recently been applied to water wave equations [19].

Many of the preceding works employ algorithms of higher order in time stepping. However, here we propose an algorithm of only second order. This is because we want a stable scheme for a long time step, which implies an implicit or semi-implicit scheme. It is possible to develop semi-implicit schemes of higher order, but these are expensive; therefore we restrict our scheme to a second order one.

As will be analysed in Section 3, our method is free of dissipation and can only introduce a numerical dispersion of $O(\Delta t^3)$. This error increases as the wavenumber increases, and therefore the Fourier components will be distorted. In the case of nonlinear dispersive waves, the energy will transfer from low wavenumbers to high wavenumbers, while, due to the dispersive terms, the rate of energy transfer may be balanced and usually a local structure such as the soliton will arise. Therefore, to ensure accuracy, the wavenumbers of a relatively broad range have to be considered and computed even though they are distorted in some way.

As explained in the last paragraph of the previous subsection, here we stress again that our algorithm has the advantage of semi-implicitness. That is, in Eq. (5), for example, the implicitness is introduced only in the linear terms. Thus the boundary value problem to be solved in each step is quite inexpensive.

3. ANALYSES OF THE SCHEME

3.1. Linear Stability Analysis

In this subsection, we analyze the stability of our scheme to the linearized KP equation

$$(u_t + \alpha u_x + u_{xxx})_x - 3\sigma^2 u_{yy} = 0 \tag{10}$$

and the linearized ZK equation

$$u_t + \alpha u_x + \Delta u_x = 0, \tag{11}$$

where $\alpha = 6 \max |u|$. The usual stability analysis process will be employed. That is, stability properties of the scheme are determined by the location of the roots of its characteristic polynomial. To this end we introduce the following definitions.

DEFINITION 1. A polynomial $\phi(z)$ all of whose roots lie strictly within the unit disk is called a Schur polynomial.

DEFINITION 2. A polynomial $\phi(z)$ all of whose roots never locate outside of the unit disk, and satisfying any root of the unit modulus that is simple, is called a simple von Neumann polynomial.

DEFINITION 3. A numerical scheme is stable if and only if its characteristic polynomial $\phi(z)$ is a simple von Neumann polynomial.

Given the polynomial $\phi(z) = \sum_{j=0}^{N} a_j z^j$ of degree N with $a_N, a_0 \neq 0$, we can obtain a polynomial $\phi_1(z)$ of degree $N-1$ by introducing $\phi^*(z) = \sum_{j=0}^{N} a_{N-j}^* z^j$ (where a^* denotes the complex conjugate of a) and defining

$$\phi_1(z) = \frac{\phi^*(0)\phi(z) - \phi(0)\phi^*(z)}{z}.$$

Now we apply the following theorem.

THEOREM 1. *$\phi(z)$ is a simple von Neumann polynomial if and only if either $|\phi^*(0)| > |\phi(0)|$ and $\phi_1(z)$ is a simple von Neumann polynomial or $\phi_1(z) \equiv 0$ and $(\mathrm{d}/\mathrm{d}z)\phi(z)$ is a Schur polynomial.*

The scheme (5) applied to the linearized Eq. (10) implies

$$\frac{\hat{u}^{n+1} - \hat{u}^{n-1}}{2\Delta t} + \mathrm{i}\alpha\xi\hat{u}^n - \mathrm{i}(\xi^3 + 3\sigma^2\eta^2/\xi)[\theta(\hat{u}^{n+1} + \hat{u}^{n-1}) + (1-2\theta)\hat{u}^n] = 0, \tag{12}$$

which derives the characteristic polynomial given as

$$\begin{aligned}\phi_{\mathrm{KP}}(z) = {} & [1 - \mathrm{i}2\Delta t\theta(\xi^3 + 3\sigma^2\eta^2/\xi)]z^2 + \mathrm{i}2\Delta t[\alpha\xi - (1-2\theta)(\xi^3 + 3\sigma^2\eta^2/\xi)]z \\ & - [1 + \mathrm{i}2\Delta t\theta(\xi^3 + 3\sigma^2\eta^2/\xi)].\end{aligned} \tag{13}$$

In view of an application of Theorem 1, it is easy to show that $|\phi^*(0)| = |\phi(0)|$ and $\phi_1(z) \equiv 0$, so that we should consider $(\mathrm{d}/\mathrm{d}z)\phi(z)$ given by

$$2[1 - \mathrm{i}2\Delta t\theta(\xi^3 + 3\sigma^2\eta^2/\xi)]z + \mathrm{i}2\Delta t[\alpha\xi - (1-2\theta)(\xi^3 + 3\sigma^2\eta^2/\xi)].$$

The requirement that this polynomial be a Schur polynomial demands that

$$1 + 4\theta^2(\Delta t)^2(\xi^3 + 3\sigma^2\eta^2/\xi)^2 > (\Delta t)^2[\alpha\xi - (1-2\theta)(\xi^3 + 3\sigma^2\eta^2/\xi)]^2$$

or

$$P_\theta(\xi, \eta) > 0, \tag{14}$$

where

$$P_\theta(\xi, \eta) \equiv 1 + (\Delta t)^2[(4\theta - 1)\xi^2(\xi^2 + 3\sigma^2\eta^2/\xi^2)^2 + 2\alpha(1-2\theta)\xi^2(\xi^2 + 3\sigma^2\eta^2/\xi^2) - \alpha^2\xi^2]. \tag{15}$$

It is easily shown that $P_\theta(\xi, \eta)$ can be rewritten as

$$P_\theta(\xi, \eta) = (\Delta t)^2(4\theta - 1)\left[(\xi^3 + 3\sigma^2\eta^2/\xi) + \alpha\frac{(1-2\theta)\xi}{4\theta - 1}\right]^2 + 1 - 2(\Delta t)^2\alpha^2\xi^2\frac{10\theta^2 - 6\theta + 1}{(4\theta - 1)^2}. \tag{16}$$

Furthermore, assuming $\theta > \frac{1}{4}$, from Eq. (14) and (16), we can get a necessary stability condition for the scheme (12), which is

$$\Delta t < C_1(\theta)\frac{1}{|\alpha|\,|\xi_{L/2}|}, \tag{17}$$

where the function $C_1(\theta)$ is given by

$$C_1(\theta) = \frac{(4\theta - 1)}{\sqrt{2(10\theta^2 - 6\theta + 1)}}.$$

Figure 1 illustrates the curve $C_1(\theta)$ versus θ for $\frac{1}{4} \le \theta \le 1$.

Similarly, for the linearized scheme of the ZK equation

$$\frac{\hat{u}^{n+1} - \hat{u}^{n-1}}{2\Delta t} + \mathrm{i}\alpha\xi\hat{u}^n - \mathrm{i}(\xi^3 + \eta^2\xi)[\theta(\hat{u}^{n+1} + \hat{u}^{n-1}) + (1-2\theta)\hat{u}^n] = 0, \tag{18}$$

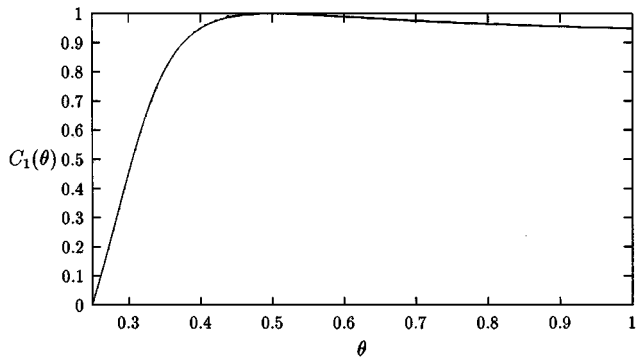

FIG. 1. The curve $C_1(\theta)$ versus θ.

we have its stability polynomial $\phi(z)$,

$$\phi_{\mathrm{ZK}}(z) = [1 - \mathrm{i}2\Delta t\theta(\xi^3 + \eta^2\xi)]z^2 + \mathrm{i}2\Delta t[\alpha\xi - (1-2\theta)(\xi^3 + \xi\eta^2)]z - [1 + \mathrm{i}2\Delta t\theta(\xi^3 + \eta^2\xi)]. \quad (19)$$

The same procedure as above gives the requirement for the linear stability as

$$1 + (\Delta t)^2[(4\theta - 1)\xi^2(\xi^2 + \eta^2)^2 + 2\alpha(1-2\theta)\xi^2(\xi^2 + \eta^2) - \alpha^2\xi^2] > 0. \quad (20)$$

We note that in the interested range $\frac{1}{4} \le \theta \le \frac{1}{2}$,

$$Q_\theta(\xi) \equiv 1 + \Delta t^2[(4\theta - 1)\xi^6 + 2\alpha(1-2\theta)\xi^4 - \alpha^2\xi^2] \ge 0 \quad (21)$$

implies Eq. (20) is satisfied. For $\theta > \frac{1}{4}$ the positive ξ^* fulfilling

$$\xi^{*2} = \frac{\sqrt{16\theta^2 - 4\theta + 1} - 2(1-2\theta)}{3(4\theta - 1)}\alpha \quad (22)$$

minimizes $Q_\theta(\xi)$.

Calculation gives the minimum as

$$m_\theta \equiv \frac{-2[(16\theta^2 - 4\theta + 1)^{3/2} + (64\theta^3 - 24\theta^2 - 6\theta + 1)]}{27(4\theta - 1)^2}\alpha^3. \quad (23)$$

The polynomial $Q_{1/4}(\xi)$ attains its minimum $-\alpha^3/4$ at $\xi^{*2} = \alpha/2$. Note that this is consistent with the limit of (22)–(23) when $\theta \to \frac{1}{4}$. Consequently, for the usual case of $\xi_1 < \xi^* < \xi_{L/2}$, a necessary stability condition for the scheme (18) of the ZK equation is

$$(\Delta t)^2 < \frac{C_2(\theta)}{\alpha^3}, \quad (24)$$

where the function $C_2(\theta)$ is given by

$$C_2(\theta) = \frac{27(4\theta - 1)^2}{2[(16\theta^2 - 4\theta + 1)^{3/2} + (64\theta^3 - 24\theta^2 - 6\theta + 1)]}.$$

Figure 2 illustrates the curve $C_2(\theta)$ versus θ for $\frac{1}{4} \le \theta \le \frac{1}{2}$.

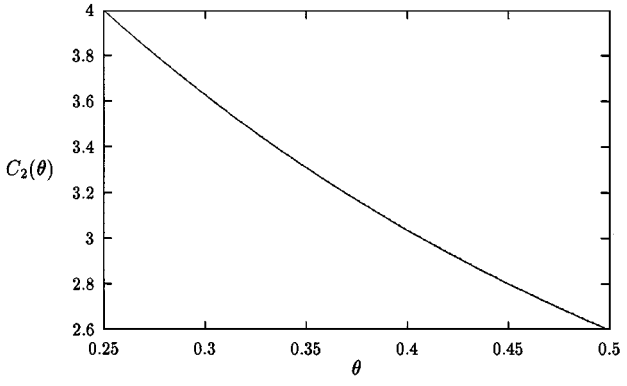

FIG. 2. The curve $C_2(\theta)$ versus θ.

Moreover assume the roots of $\phi(z)$ for Eqs. (13) and (19) be z_1 and z_2. When the polynomial is von Neumann, from the fact that $|z_1|\,|z_2| = 1$ and $|z_{1,2}| \le 1$, we can easily see that $|z_1| = |z_2| = 1$. Therefore, the schemes (5) and (6) are conservative.

We summarize the above results in the following theorems.

THEOREM 2. *For the linear periodic initial value problem*

$$\begin{aligned}
&(u_t + \alpha u_x + u_{xxx})_x - 3\sigma^2 u_{yy} = 0, && (x, y) \times t \in \Omega \times [0, \infty),\\
&u(x, y, 0) = u_0(x, y), && (x, y) \in \Omega,\\
&u(x, y, t) = u(x + W_x, y, t),\\
&u(x, y, t) = u(x, y + W_y, t), && (x, y) \times t \in \mathbf{R}^2 \times [0, \infty),
\end{aligned}$$

where $\Omega = [0, W_x] \times [0, W_y]$, $\alpha \in \mathbf{R}^+$, *the spectral scheme*

$$\frac{\hat{u}^{n+1} - \hat{u}^{n-1}}{2\Delta t} + \mathrm{i}\alpha\xi\hat{u}^n - \mathrm{i}(\xi^3 + 3\sigma^2\eta^2/\xi)[\theta(\hat{u}^{n+1} + \hat{u}^{n-1}) + (1 - 2\theta)\hat{u}^n] = 0$$

is conservative and stable provided that $\theta > \frac{1}{4}$ *and the estimation* (17) *holds for the time step size.*

THEOREM 3. *For the linear periodic initial value problem*

$$\begin{aligned}
&u_t + \alpha u_x + \Delta u_x = 0, && (x, y) \times t \in \Omega \times [0, \infty),\\
&u(x, y, 0) = u_0(x, y), && (x, y) \in \Omega,\\
&u(x, y, t) = u(x + W_x, y, t),\\
&u(x, y, t) = u(x, y + W_y, t), && (x, y) \times t \in \mathbf{R}^2 \times [0, \infty),
\end{aligned}$$

where $\Omega = [0, W_x] \times [0, W_y]$, $\alpha \in \mathbf{R}^+$, *the spectral scheme*

$$\frac{\hat{u}^{n+1} - \hat{u}^{n-1}}{2\Delta t} + \mathrm{i}\alpha\xi\hat{u}^n - \mathrm{i}(\xi^3 + \xi\eta^2)[\theta(\hat{u}^{n+1} + \hat{u}^{n-1}) + (1 - 2\theta)\hat{u}^n] = 0$$

is conservative and stable provided that $\frac{1}{4} \le \theta \le \frac{1}{2}$ *and the estimation* (24) *holds for the time step size.*

3.2. Accuracy and Numerical Dispersion

The methods we are concerned with solve the problem by Fourier analysis in space and by the finite difference method in time. To examine errors incurred by the spectral method considered here, we ignore spatial discretization errors and consider only errors associated with the temporal discretization. We can easily conclude that the temporal discretization of our schemes (5)–(6) are of order $O(\Delta t^2)$.

Since our schemes for Eqs. (1) and (2) are conservative, the truncation error contains only dispersion errors. For wave simulations, only long waves can be approximated well. Thus, the dispersion error of the higher frequency components is of little significance, and the main interest is in the sufficiently small ξ and η. We should confirm that numerical dispersion does not exceed physical dispersion.

We next derive the numerical dispersion in time for the methods (5) and (6). Define ψ_e to be the analytical dispersion in one time step; then it can be shown that

$$\psi_e = \Delta t(-\alpha\xi + A), \tag{25}$$

where for the KP equation $A = \xi^3 + 3\sigma^2\eta^2/\xi$, and for the ZK equation $A = \xi^3 + \xi\eta^2$.

Assume the roots for Eqs. (13) and (19) to be $e^{i\psi_i}$, $i = 1, 2$; then we have the numerical dispersion $\psi = \max(\psi_1, \psi_2)$.

For small ξ, η, Taylor's series expansion yields the root with the maximum phase angle

$$z_{\max} = 1 + \frac{\Delta t^2}{2}(\alpha^2\xi^2 - 2\alpha\xi(1-2\theta)A - (4\theta-1)A^2) - i\Delta t(\alpha\xi - A).$$

Therefore the numerical dispersion is given by

$$\psi = \tan^{-1}\frac{\Im(z_{\max})}{\Re(z_{\max})}. \tag{26}$$

Again, by virtue of Taylor's series expansion, we obtain

$$\psi = \Delta t(-\alpha\xi + A) + \frac{(\Delta t)^3}{6}(\alpha\xi - A)^2(\alpha\xi + (12\theta - 1)A) + O(\Delta t^4). \tag{27}$$

Combining (27) with (25) leads to the numerical dispersion error of the methods (5) and (6) to be

$$\psi - \psi_e = \frac{(\Delta t)^3}{6}(\alpha\xi - A)^2(\alpha\xi + (12\theta - 1)A) + O(\Delta t^4). \tag{28}$$

We comment on the numerical dispersion errors. First, the ratio of the numerical dispersion to the physical dispersion of the schemes (5) and (6) is of the order $O(\Delta t^2)$, which is very small. Second, the dispersion error is proportional to the parameter θ. Henceforth, provided the method is stable, the smaller θ is, the smaller the dispersion error is. The numerical results in the following section confirm this result.

4. NUMERICAL EXPERIMENTS

Here we will show several numerical experiments to illustrate the efficiency of our method. We use the FFT subroutines DFOUR in the *Numerical Recipe* library [18]. Computations are performed on a Sun UltraSPARC workstation using Fortran 77 4.0 with the double precision arithmetic.

4.1. KP Equation

In the case of $\sigma^2 = 1$, Eq. (1) is usually called the KPI equation, whereas in the case of $\sigma^2 = -1$, it is called the KPII equation. For the KPI equation, there exists a lump-type solution which decay as $O(1/r^2)$, $r^2 = x^2 + y^2$ when $r \to \infty$. This lump-type solution can be expressed as

$$u(x, y, t) = 4\frac{\{-[x + \lambda y + 3(\lambda^2 - \mu^2)t]^2 + \mu^2(y + 6\lambda t)^2 + 1/\mu^2\}}{\{[x + \lambda y + 3(\lambda^2 - \mu^2)t]^2 + \mu^2(y + 6\lambda t)^2 + 1/\mu^2\}^2}. \tag{29}$$

It is also shown [13] that the KPII equation admits a large family of solutions of the form

$$u(x, y, t) = 2\frac{\partial^2}{\partial x^2} \ln \theta(\phi_1, \ldots, \phi_N \mid Z), \tag{30}$$

where $\theta(\phi_1, \ldots, \phi_N \mid Z)$ is a Riemann theta function of genus N, which may be defined as the Fourier series

$$\theta(\phi_1, \ldots, \phi_N \mid Z) = \sum_{m_1, \ldots, m_N} \exp\left(-\frac{1}{2} m^T Z m + \mathrm{i} m^T \phi\right), \tag{31}$$

where $m^T = (m_1, \ldots, m_N)$ and Z is a $N \times N$ symmetric, real, positive-definite Riemann matrix. Equation (30) is also called the N-phase solution of the KP equation. The phase variable ϕ is defined by

$$\phi_j = \mu_j x + \nu_j y + \omega_j t + \phi_{j,0}, \qquad j = 1, \ldots, N. \tag{32}$$

Two-phase solution of the KP equation is first computed in [22]. Recent comparisons with experiments [8, 9] show that the family of two-phase solutions of KP equations describes waves in shallow water with surprising accuracy.

Every two-phase solution is spatially periodic in two directions, but it need not be periodic in either the x- or y-direction. A subset of solutions that are periodic in both x and y are symmetric solutions. A symmetric two-phase solution has three independent parameters (because it requires $z_{11} = z_{22}$, $\mu_1 = \mu_2$, and $\nu_1 = -\nu_2$). Symmetric solutions propagate purely in the x-direction.

The lump-type soliton problems for the KPI equation and the two-phase solution for the KPII equation are both solved numerically using our method (5).

4.1.1. *KPI Equation*

The lump-type initial condition used for the KPI equation is

$$u(x, y, 0) = 4\frac{\left\{-(x - x_0)^2 + \mu^2 (y - y_0)^2 + 1/\mu^2\right\}}{\left\{(x - x_0)^2 + \mu^2 (y - y_0)^2 + 1/\mu^2\right\}^2}. \tag{33}$$

We adopt the periodic boundary conditions and compute on a domain $\Omega = [0, 40] \times [0, 40]$ with the parameters $\mu^2 = 1.0$, $x_0 = 20.0$, $y_0 = 20.0$.

According to (29), this lump-type solitary wave will move to the positive x-direction with velocity $3\mu^2$. Figure 3 shows the initial condition and the numerical solution at time $t = 2.0$. Stable propagation of the lump-type solitary wave is observed without any deformation.

Collisions of two lump-type solitary waves are also examined in the same way. We adopt the initial conditions

$$u(x, y, 0) = 4\sum_{i=1}^{2} \frac{\left\{-[(x - x_{0,i}) + \lambda_i (y - y_{0,i})]^2 + \mu_i^2 (y - y_{0,i})^2 + 1/\mu_i^2\right\}}{\left\{[x - x_{0,i} + \lambda_i (y - y_{i,0})]^2 + \mu_i^2 (y - y_{0,i})^2 + 1/\mu_i^2\right\}^2} \tag{34}$$

with two sets of values for the parameters

$$x_{0,1} = 10.0, \qquad x_{0,2} = 18.0, \qquad y_{0,1} = y_{0,2} = 10.0,$$
$$\mu_1^2 = 1.5, \qquad \mu_2^2 = 0.75, \qquad \lambda_1 = \lambda_2 = 0.0,$$

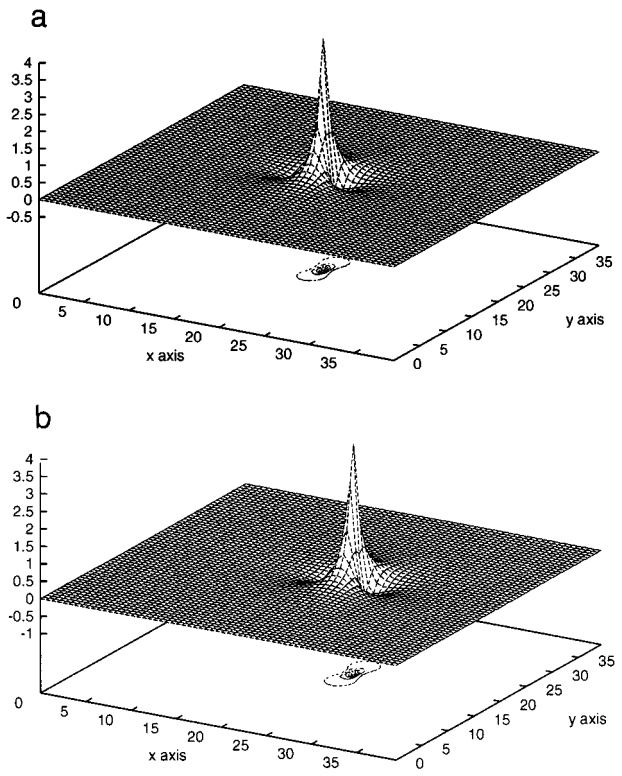

FIG. 3. Stable evolution of one lump-type solitary wave ($\Delta x = 0.3125$, $\Delta t = 0.01$). (a) $t = 0.0$, (b) $t = 2.0$.

and

$$x_{0,1} = x_{0,2} = 10.0, \qquad y_{0,1} = 10.0, \qquad y_{0,2} = 30.0,$$
$$\mu_1^2 = \mu_2^2 = 1.0, \qquad \lambda_1 = 1.0, \qquad \lambda_2 = -1.0.$$

According to (29), Eq. (34) represents two lump-type solitary waves initially located at $(x_{0,1}, y_{0,1})$ and $(x_{0,2}, y_{0,2})$, respectively. The first one moves with velocities $v_{1,x} = 3(\lambda_1^2 + \mu_1^2)$ in the positive x-direction and $v_{1,y} = -6\lambda_1$ in the positive y-direction, whereas the second one moves with velocities $v_{2,x} = 3(\lambda_2^2 + \mu_2^2)$ and $v_{2,y} = -6\lambda_2$. For the first set, values of the parameters are $v_{1,x} = 4.5$, $v_{2,x} = 2.25$ and $v_{1,y} = v_{2,y} = 0$. Henceforth, the first lump-type solitary wave initially at (10.0, 20.0) moves faster than the second one initially at (18.0, 20.0); therefore, it will catch up with and have a "direct collision" with the second one. The numerical solutions are shown in Fig. 4. It is amazing that the two lump solitary waves undergo an "inelastic collision"and break into two more lump solitary waves with equal amplitudes. They move with velocities $v_{1,x} = v_{2,x} \approx 3.125$, $v_{1,y} = -v_{2,y} \approx 1.094$. This phenomenon is the same as in [2]. But this time the ripples in the numerical solution in [2] disappear due to the high accuracy of our spectral method. The above computation is implemented on a 256×256 grid with $\Delta t = 0.004$.

For the second set, values of the parameters are $v_{1,x} = v_{2,x} = 6.0$ and $v_{1,y} = -v_{2,y} = -6.0$. So these two lump-type solitary waves move close with an angle of $\pi/2$ and encounter an "indirect collision" afterwards. Figure 5 gives the numerical results via the scheme (5) on a 128×128 grid with $\Delta t = 0.01$.

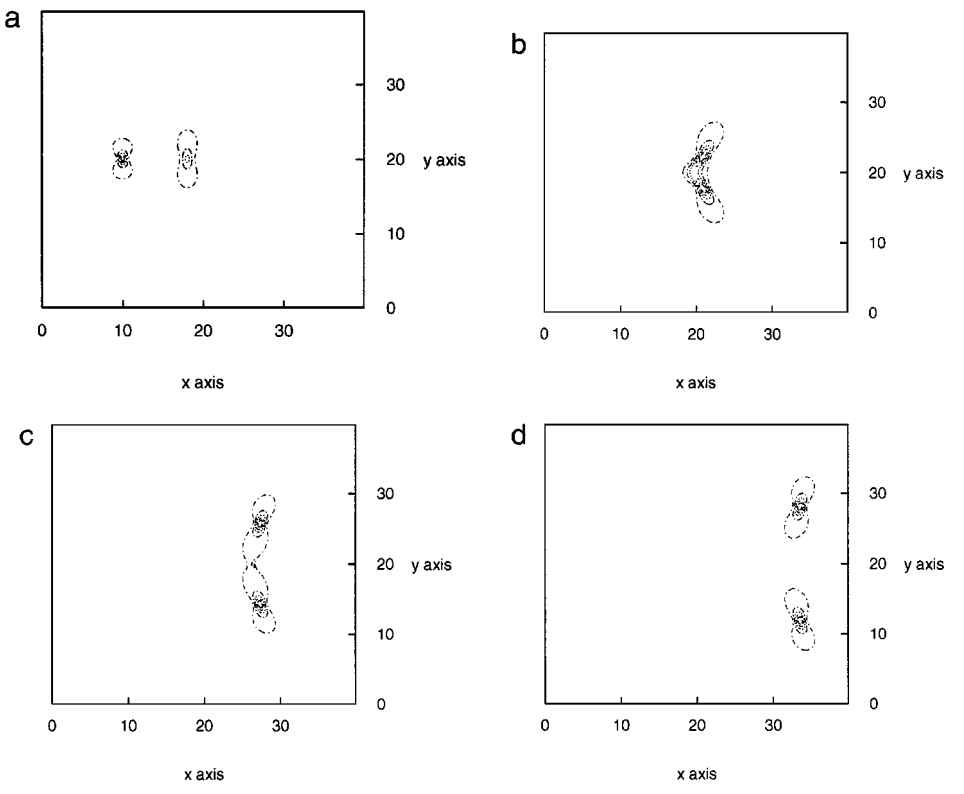

FIG. 4. Contour curves for a direct collision of two pulses. (a) $t = 0.0$, (b) $t = 2.0$, (c) $t = 4.0$, (d) $t = 6.0$.

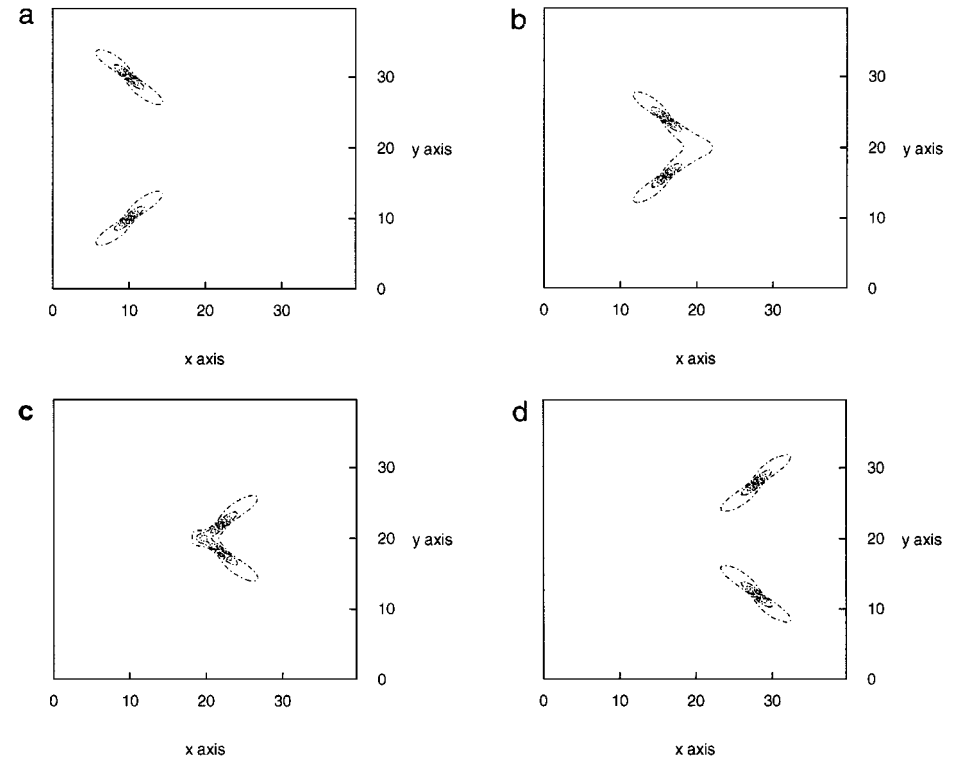

FIG. 5. Contour curves for an indirect collision of two pulses. (a) $t = 0.0$, (b) $t = 2.0$, (c) $t = 4.0$, (d) $t = 6.0$.

It is seen that these two lump solitary waves undergo an "elastic collision" and cross each other with changes neither in their shapes nor in the phase shift. What is the mechanism for the interactions of the two lump-type solitary waves? This remains a topic to be investigated.

4.1.2. *KPII Equation*

As in [26], the two-phase solutions of the KPII equation with two sets of values for the parameters and proper initial phases provide us the initial conditions in our computations. They are

$$\begin{gathered} z_{11} = z_{22} = 1.0, \qquad z_{12} = 0.15, \mu_1 = \mu_2 = 0.25, \\ \nu_1 = -\nu_2 = 0.25269207053125, \qquad \omega_1 = \omega_2 = -1.5429032317052, \end{gathered} \tag{35}$$

and

$$\begin{gathered} z_{11} = z_{22} = 1.0, \quad z_{12} = 0.15, \qquad \mu_1 = \mu_2 = 0.25, \\ \nu_1 = 0.5053841410625, \qquad \nu_2 = 0.0, \\ \omega_1 = -3.8416214020425, \qquad z\omega_2 = -0.7766638415928. \end{gathered} \tag{36}$$

We take one period in the x-direction and two periods in the y-direction. Thus the computation domain is $[2\pi/\mu_1, 4\pi/\nu_1]$.

Figure 6 shows the surface plot and a contour plot for the initial conditions with the parameters given by (35), which is an example for a symmetric two-phase solution of the KPII equation. The numerical solution on a 128 by 128 grid with $\Delta t = 0.005$ at time $t = 1.0$ is shown in Fig. 7.

With the same time step size $\Delta t = 0.005$, comparisons with analytical solutions in the standard L_p-norms over the two-dimensional spatial mesh and one of the conservative quantities $I = \frac{1}{2}\int\int u^2(x, y)\, dx\, dy$ are exhibited in Table 1 with $\theta = \frac{1}{3}, \frac{1}{2}$, and $\frac{2}{3}$. The relative errors

$$\frac{\|u_{l,m} - u(l\Delta x, m\Delta y)\|_p}{\|u(l\Delta x, m\Delta y)\|_p} \tag{37}$$

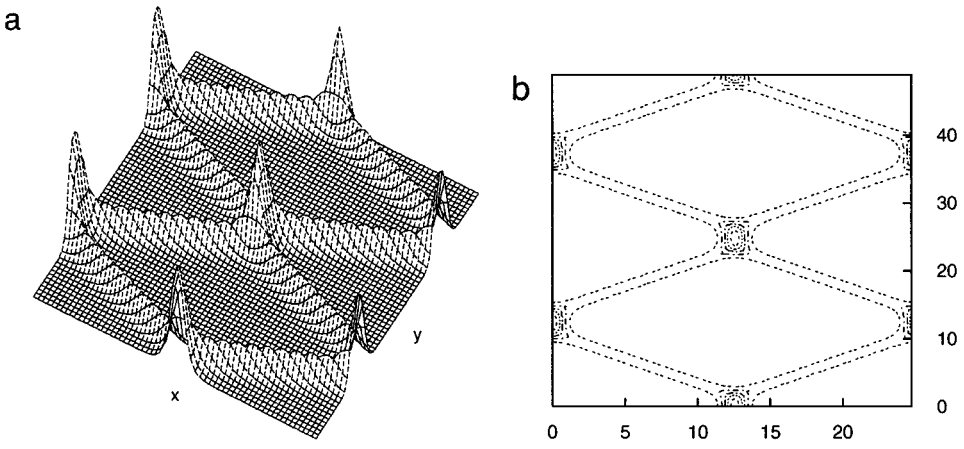

FIG. 6. Initial conditions for the two-phase solution ($\nu_2 = -\nu_1$). (a) Profile. (b) Contour curves.

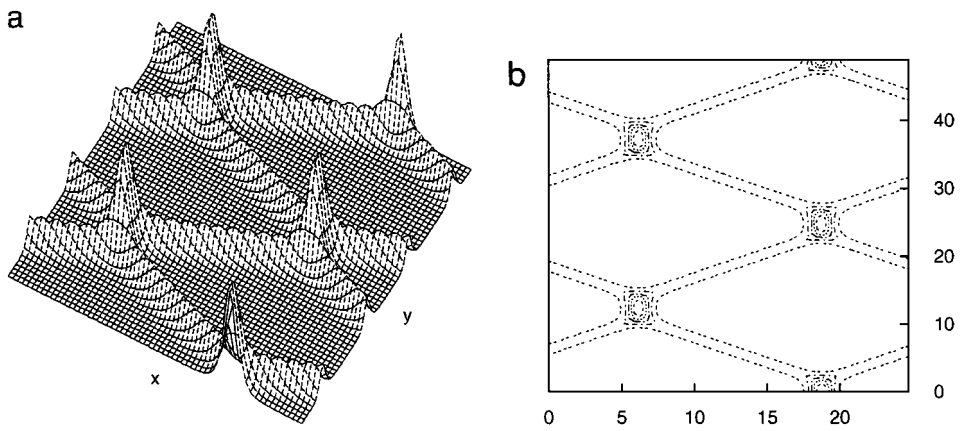

FIG. 7. Numerical solution for the two-phase solution ($\nu_2 = -\nu_1$) at $t = 1.0$. (a) Profile. (b) Contour curves.

are computed for $p = 1, 2, \infty$. $E = |\bar{I} - I|/|I|$ indicates the relative error of the approximate values in the conserved quantities. Here $\bar{I}$ stands for the computed value of I. Simpson's rule was employed for the numerical quadrature of the integrals.

Similarly, Figs. 8 and 9 and Table 2 show the initial conditions, numerical solution at time $t = 1.0$, and relative errors in L_p for $p = 1, 2, \infty$ and conservative quantity I for the parameters (36) with $\Delta t = 0.005$.

To make comparisons with the Wineberg scheme, we solve numerically the above two problems again using the schemes (5) and (9). Similarly as in Taha and Ablowitz [23], we fix the L_2-norm at the terminating time $t = 1.0$, adjusting the discretization parameters so that they minimize the CPU time. Tables 3 and 4 show these results. It can be seen that our method is more efficient than the Wineberg scheme (9). Especially, one of the conserved quantities I is very well preserved.

TABLE 1
Relative Errors in the L_p-norms and the Conservative Quantity E for the Method (5) ($\nu_2 = -\nu_1$)

Grid	θ	t	L_1	L_2	L_∞	$E(\times 10^{-3})$
64×64	$\frac{1}{3}$	0.5	0.0046	0.0061	0.0160	0.106
64×64	$\frac{1}{3}$	1.0	0.0069	0.0099	0.0236	0.317
128×128	$\frac{1}{3}$	0.5	0.0027	0.0033	0.0044	0.015
128×128	$\frac{1}{3}$	1.0	0.0041	0.0048	0.0049	0.020
64×64	$\frac{1}{2}$	0.5	0.0049	0.0066	0.0166	0.127
64×64	$\frac{1}{2}$	1.0	0.0085	0.0113	0.0268	0.390
128×128	$\frac{1}{2}$	0.5	0.0036	0.0044	0.0060	0.020
128×128	$\frac{1}{2}$	1.0	0.0055	0.0064	0.0065	0.022
64×64	$\frac{2}{3}$	0.5	0.0056	0.0017	0.0171	0.135
64×64	$\frac{2}{3}$	1.0	0.0090	0.0117	0.0257	0.337
128×128	$\frac{2}{3}$	0.5	0.0047	0.0055	0.0075	0.037
128×128	$\frac{2}{3}$	1.0	0.0069	0.0079	0.0082	0.032

TABLE 2
Relative Errors in the L_p-norms and the Conservative Quantity E for the Method (5) ($\nu_2 = 0$)

Grid	θ	t	L_1	L_2	L_∞	$E(\times 10^{-3})$
64×64	$\frac{1}{3}$	0.5	0.0060	0.0104	0.0269	0.262
64×64	$\frac{1}{3}$	1.0	0.0102	0.0156	0.0373	0.623
128×128	$\frac{1}{3}$	0.5	0.0048	0.0063	0.0085	0.019
128×128	$\frac{1}{3}$	1.0	0.0079	0.0083	0.0091	0.022
64×64	$\frac{1}{2}$	0.5	0.0074	0.0120	0.0257	0.284
64×64	$\frac{1}{2}$	1.0	0.0113	0.0185	0.0401	0.766
128×128	$\frac{1}{2}$	0.5	0.0059	0.0089	0.0104	0.032
128×128	$\frac{1}{2}$	1.0	0.0094	0.0117	0.0155	0.032
64×64	$\frac{2}{3}$	0.5	0.0077	0.0141	0.0232	0.245
64×64	$\frac{2}{3}$	1.0	0.0114	0.0181	0.0265	0.288
128×128	$\frac{2}{3}$	0.5	0.0069	0.0121	0.0121	0.046
128×128	$\frac{2}{3}$	1.0	0.0113	0.0164	0.0227	0.065

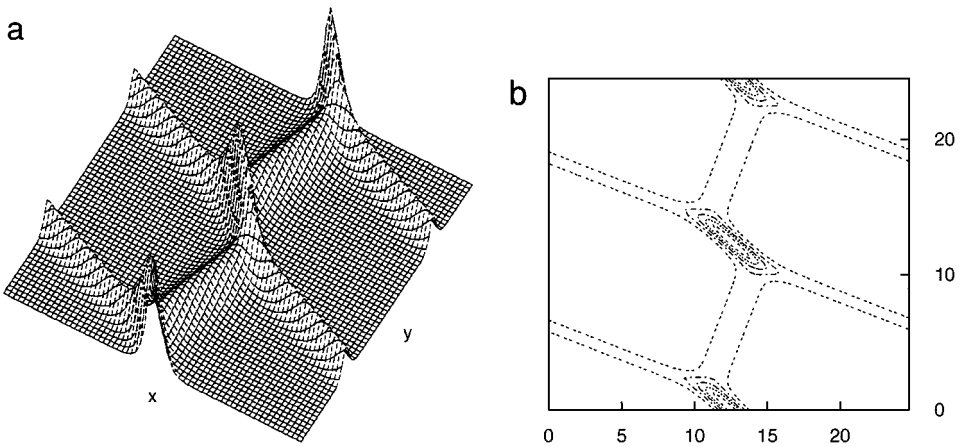

FIG. 8. Initial condition for the two-phase solution ($\nu_2 = 0$). (a) Profile. (b) Contour curves.

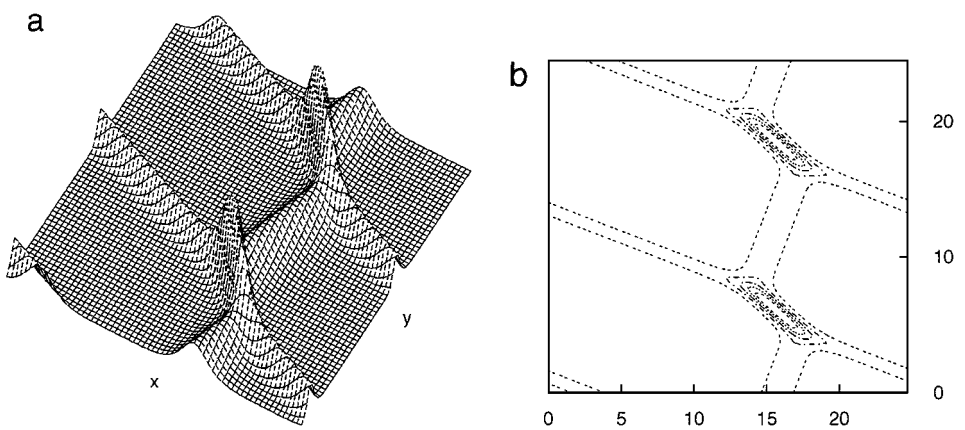

FIG. 9. Numerical solution for the two-phase solution ($\nu_2 = 0$) at $t = 1.0$. (a) Profile. (b) Contour curves.

TABLE 3
Comparison of Computing Times for Two-Phase Solution ($\nu_2 = -\nu_1$)

Scheme	Δt	CPUs	L_1	L_2	L_∞	$E(\times 10^{-3})$
Wineberg						
$R=2$	0.0027	336.4	0.0037	0.0047	0.0044	0.886
$R=3$	0.006	242.4	0.0044	0.0050	0.0050	3.138
Scheme (5)						
$\theta=\frac{1}{3}$	0.005	178.6	0.0041	0.0048	0.0049	0.002
$\theta=\frac{1}{2}$	0.0044	202.1	0.0042	0.0049	0.0050	0.016

4.2. ZK Equation

A cylindrically symmetric solitary solution was obtained, and its evolutions as well as interactions were investigated numerically [11]. This type of solitary solution, also called the bell-shaped pulse, can be expressed as

$$u(x, y, t) = \frac{c}{3}\sum_{n=1}^{10} a_{2n}\left(\cos\left(2n \operatorname{arccot}\left(\frac{\sqrt{c}}{2}r\right)\right) - 1\right), \tag{38}$$

where c is the velocity of the solitary wave solution and $r = \sqrt{(x-ct)^2 + y^2}$. The coefficients are collected in Table 5.

In order to show the effectiveness of the scheme (6), several examples for the propagation and the interactions of such bell-shaped pulses are computed on a domain $\Omega = [0, 32] \times [0, 32]$ with periodic boundary conditions.

First, a single bell-shaped pulse with velocity $c = 4.0$ initially located at (16.0, 16.0) is assigned as the initial condition. Figure 10 shows the initial condition and the numerical solution at time $t = 2.0$. It is observed that this single pulse propagates stably like a soliton without any deformation.

Second, two similar pulses ($c_1 = 4.4$, $c_2 = 4.0$) are initially located at (16.0, 16.0) and (26.0, 16.0), respectively. This case is called "direct collision" in [11], because the centers of the two pulses are situated on the same line with $y =$ const. Figure 11 shows the contour plot. It is seen that the collision is almost elastic.

Results of "deviated collision," i.e., collision of two pulses with their centers slightly shifted to the y-direction, are shown in Fig. 12. Two similar pulses ($c_1 = 4.4$, $c_2 = 4.0$) are

TABLE 4
Comparison of Computing Times for Two-Phase Solution ($\nu_2 = 0$)

Scheme	Δt	CPUs	L_1	L_2	L_∞	$E(\times 10^{-3})$
Wineberg						
$R=2$	0.0024	369.8	0.0052	0.0047	0.0046	0.865
$R=3$	0.0038	339.5	0.0036	0.0049	0.0046	1.504
Scheme (5)						
$\theta=\frac{1}{3}$	0.0038	199.4	0.0045	0.0048	0.0053	0.008
$\theta=\frac{1}{2}$	0.0032	214.2	0.0038	0.0048	0.0063	0.005

TABLE 5
Coefficients for the Solitary Wave Solution of the ZK Equation

n:	1	2	3	4	5
a_{2n}:	−1.25529873	0.21722635	0.06452543	0.00540862	−0.00332515
n:	6	7	8	9	10
a_{2n}:	−0.00281281	−0.00138352	−0.00070289	−0.00020451	−0.00003053

located at (16.0, 14.0) and (26.0, 16.0) initially. From Fig. 12, we can see that the two pulses exchange their amplitudes through the interaction of their tails without merging with each other. Ripples are generated obviously after deviated collision. All the results obtained here are consistent with ones in [11]; however, through the computations, we could use a larger time step size $\Delta t = 0.01$, which must lead to numerical instability for the explicit scheme used in [11].

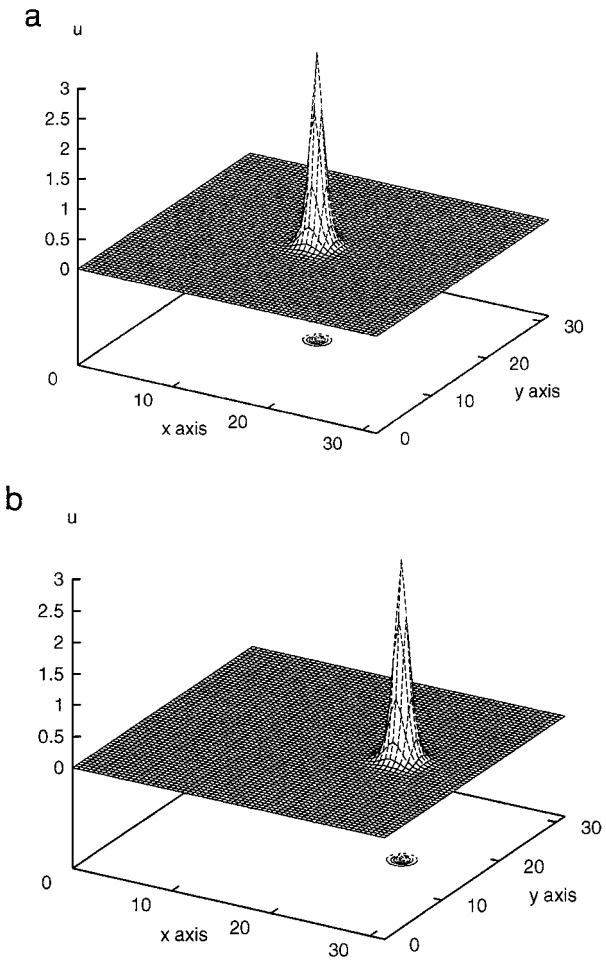

FIG. 10. Evolution of a single bell-shaped pulse for the ZK equation ($\Delta x = 0.25$, $\Delta t = 0.005$). (a) $t = 0.0$, (b) $t = 2.0$.

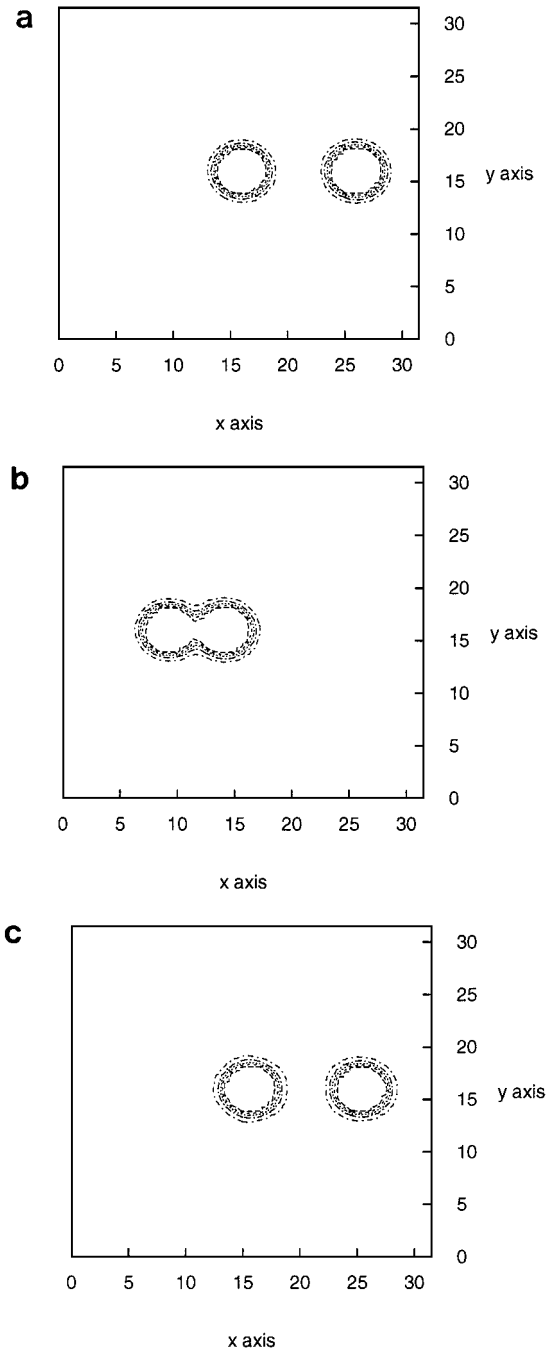

FIG. 11. Direct collision of two bell-shaped pulses ($\Delta x = 0.25$, $\Delta t = 0.01$). (a) $t = 0.0$, (b) $t = 13.0$, (c) $t = 30.0$.

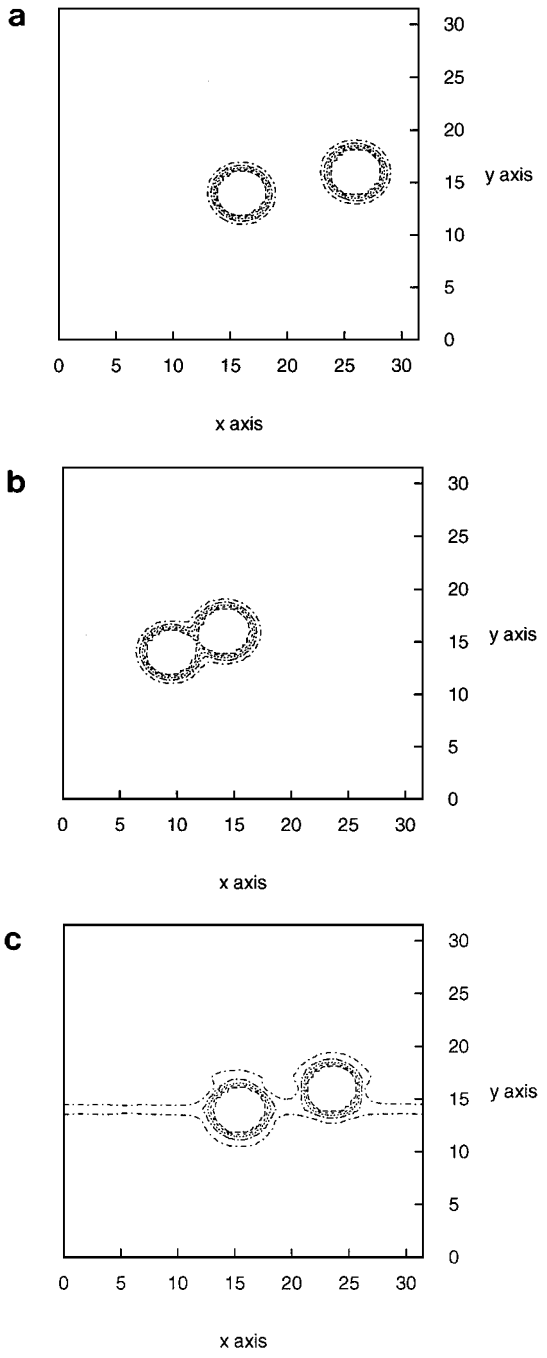

FIG. 12. Deviated collision of two bell-shaped pulses ($\Delta x = 0.25$, $\Delta t = 0.01$). (a) $t = 0.0$, (b) $t = 13.0$, (c) $t = 30.0$.

5. COMMENTS AND CONCLUSIONS

We extend the conservative spectral method for the third- and the fifth-order KdV equations [3] to several two-dimensional nonlinear wave equations, which are characterized by the linear higher order derivative terms. We employ the standard FFT to approximate the spatial derivatives, while for the time integration, we use a three-level difference scheme with a free parameter θ for the linear part and the leapfrog scheme for the nonlinear part of the equations. Henceforth, this method has the disadvantage of needing a starting procedure. However, the following merits are obtained.

1. The order of accuracy in time is of order $O(\Delta t^2)$.
2. The linear stability conditions of the proposed schemes for the KP and the ZK equations are improved compared to the corresponding explicit schemes. In particular, the stability limit of the ZK equation is much less restrictive than that of its one-dimensional analog, i.e., the KdV equation, and is independent of the number of Fourier modes.
3. The method is conservative.
4. The ratio of the numerical dispersion to the physical dispersion is of order $O(\Delta t^2)$, which is sufficiently small.
5. Although the method is semi-implicit, the computation can be implemented explicitly, and FFTs are required only twice in each time step.

Although a linearized stability analysis is not sufficient for proving stability and convergence of the corresponding nonlinear schemes, the obtained stability conditions are often sufficient in practice. We carried out many numerical experiments for the KP equation with various initial conditions, most of which are based on theoretical solutions. Numerical results show that our method for the KP equation is faster and more accurate than the method in [26]. The collisions of the two lump-type solitary waves, whose behavior is still analytically unknown, are reported and remain an interesting topic of study.

We also implemented the numerical experiments for the propagation and the collisions of the quasi-solitons for the ZK equation, as a typical example of the nonintegrable equations. A relatively large time step size is allowed and even then the same results as in [11] are obtained.

Although analyses are carried out to the schemes for the KP and the ZK equations, the same procedure can be applied to other two-dimensional nonlinear wave equations, such as the two-dimensional Benney equation. A forthcoming paper will report the numerical results for these equations.

REFERENCES

1. J. P. Boyd, *Chebyshev and Fourier Spectral Methods* (Springer-Verlag, New York, 1989).
2. B. F. Feng and T. Mitsui, A finite difference method for the Korteweg–de Vries and the Kadomtsev–Petviashvili equations, *J. Comput. Appl. Math.* **90**, 95 (1998).
3. B. F. Feng, T. Kawahara, and T. Mitsui, *A Conservative Spectral Method for the Third- and Fifth-Order Korteweg–de Vries Equations*, in preparation.
4. B. Fornberg and G. B. Whitham, A numerical and theoretical study of certain nonlinear wave phenomena, *Phil. Trans. R. Soc. London* **289**, 373 (1978).
5. B. Fornberg, *A Practical Guide to Pseudospectral Methods* (Cambridge Univ. Press, Cambridge, UK, 1996).
6. K. Goda, On instability of some finite difference schemes for the Korteweg–de Vries equation, *J. Phys. Soc. Jpn.* **39**, 229 (1975).

7. I. S. Greig and J. Ll. Morris, A hopscoth method for the Korteweg–de Vries equation, *J. Comput. Phys.* **20**, 64 (1976).
8. J. Hammack, N. Scheffner, and H. Segur, Two-dimensional periodic waves in shallow water, *J. Fluid Mech.* **209**, 567 (1989).
9. J. Hammack, D. McCallister, N. Scheffner, and H. Segur, Two-dimensional periodic waves in shallow water. 2. *J. Fluid Mech.* **285**, 95 (1995).
10. R. H. Hardin and F. D. Tappert, Applications of the split-step Fourier method to the numerical solution of nonlinear and variable coefficient wave equations, *SIAM Rev. Chronicle* **15**, 423 (1973).
11. H. Iwasaki, S. Toh, and T. Kawahara, Cylindrical quasi-solitons of the Zakharov–Kuznetsov equation, *Physica D* **43**, 293 (1990).
12. V. I. Karpman and E. M. Kruskal, Modulated waves in nonlinear dispersive media, *Sov. Phys. JETP* **28**, 277 (1969).
13. I. M. Krichever, Methods of algebraic geometry in the theory of nonlinear equations, *Russ. Math. Surveys* **32**, 183 (1977).
14. S. Melkonian and S. A. Maslowe, Two-dimensional amplitude evolution equations for nonlinear dispersive waves on thin films, *Physica D* **34**, 255 (1989).
15. D. G. Gottlieb and S. A. Orszag, *Numerical Analysis of Spectral Methods: Theory and Applications* (SIAM, Philadelphia, 1977).
16. K. Nozaki, Vortex solitons of drift waves and anomalous diffusion, *Phys. Rev. Lett.* **46**, 184 (1981).
17. V. I. Petviashvili, Red spot of Jupiter and the drift soliton in a plasma, *JETP Lett.* **32**, 619 (1980).
18. W. H. Press, S. A. Teukolsky, W. T. Vetterling, and B. P. Flannery, *Numerical Recipes in Fortran 77* (Cambridge Univ. Press, Cambridge, UK, 1992), 2nd ed., p. 518.
19. B. F. Sanders, N. K. Katopodes, and J. P. Boyd, Spectral modeling of nonlinear dispersive waves, *J. Hydraulic Eng. ASCE* **124**, 2 (1998).
20. J. M. Sanz-Serna and I. Christie, Petrov–Galerkin methods for nonlinear dispersive waves, *J. Comput. Phys.* **39**, 94 (1981).
21. J. Satsuma and N. Yajima, Initial value problems of one-dimensional self-modulation of nonlinear waves in dispersive media, *Prog. Theor. Phys. Suppl.* **55**, 284 (1974).
22. H. Segur and A. Finkel, An analytical model of periodic waves in shallow water, *Stud. Appl. Math.* **73**, 183 (1985).
23. T. R. Taha and M. J. Ablowitz, Analytical and numerical aspects of certain nonlinear evolution equations. 3. Numerical Korteweg–de Vries equation, *J. Comput. Phys.* **55**, 231 (1984).
24. S. Toh, H. Iwasaki, and T. Kawahara, Two-dimensional localized pulses of a nonlinear equation with dissipation and dispersion, *Phys. Rev. A* **40**, 5472 (1989).
25. A. C. Vilegenthart, On finite difference methods for the Korteweg–de Vries equation, *J. Eng. Math.* **5**, 137 (1971).
26. S. B. Wineberg, J. F. McGrath, E. F. Gabl, L. R. Scott, and C. E. Southwell, Implicit spectral methods for wave propagation problems, *J. Comput. Phys.* **97** 311 (1991).
27. N. Yajima and A. Outi, A new example of stable solitary waves, *Prog. Theor. Phys.* **45**, 1997 (1971).
28. N. J. Zabusky and M. D. Kruskal, Interaction of "solitons" in a collisionless plasma and the recurrence of initial states, *Phys. Rev. Lett.* **15**, 240 (1965).
29. V. E. Zakharov and E. A. Kuznetsov, Three-dimensional solitons, *Sov. Phys. JETP* **39**, 285 (1974).